

RESEARCH

Open Access



# Genomic diversity of *Capillovirus uniheveae* (*Betaflexiviridae*) infecting *Hevea brasiliensis* Muell. Arg. in Hainan, China

Hao Wang<sup>1</sup>, Ruibai Zhao<sup>1</sup>, Xi Huang<sup>1</sup>, Hongxing Wang<sup>1\*</sup> and Xianmei Cao<sup>1\*</sup>

## Abstract

**Background** Rubber tree (*Hevea brasiliensis* Muell. Arg.) is a significant commercial crop in tropical areas worldwide, with rubber production threatened by Tapping Panel Dryness (TPD). Rubber tree virus 1 (*Capillovirus uniheveae*; RTV1) was identified in rubber tree samples with TPD symptoms through RNA-seq. However, its genetic diversity may have hindered the detection of RTV1 via RT-PCR, complicating the further identification of RTV1 as the causative agent of TPD. To assess RTV1 prevalence and genomic diversity, rubber tree bark samples with TPD syndrome were collected from various sites in Hainan, China, for RNA-seq and RTV1 genome determination.

**Results** Twenty complete RTV1 genomes were determined from 22 samples with TPD syndrome via RNA-seq and RT-PCR. Using degenerate primers based on conserved sequences in the 3'- and 5'-UTR, 20 complete RTV1 genomes were identified directly from 48 trees affected by TPD via RT-PCR. The 40 RTV1 genome sequences showed significant variations, particularly in the RdRp domain. Phylogenetic analysis of full-genome nucleotide sequences divided RTV1 isolates into three phylogroups (A, B, and C), with phylogroup A being the most prevalent (67.5%). Similar results were observed based on RdRp and CP phylogenetic analysis. Additionally, mixed infections with different genotypes were identified in the same tree. Notably, no genetic recombination was observed among different phylogroups, while ten recombination events were identified within phylogroup A.

**Conclusions** RTV1 was identified in approximately 50% of samples with TPD syndrome collected in Hainan, China, with phylogroup A being the most prevalent. Considerable variations were observed in RTV1 nucleotide sequences among different phylogroups. These findings lay a foundation for accurate diagnostics, etiological characterization, and elucidation of the evolutionary relationships of RTV1 populations, providing a strong guarantee for obtaining virus-free rubber tree seedlings, and promoting the healthy and sustainable development of rubber tree plantations.

**Keywords** *Hevea brasiliensis*, RTV1, Genetic diversity, TPD, RNA-seq, RT-PCR

\*Correspondence:

Hongxing Wang  
wanghongxing@hainanu.edu.cn  
Xianmei Cao  
18217924350@163.com

<sup>1</sup>School of Breeding and Multiplication (Sanya Institute of Breeding and Multiplication), Hainan University, Sanya 572025, China



© The Author(s) 2025. **Open Access** This article is licensed under a Creative Commons Attribution-NonCommercial-NoDerivatives 4.0 International License, which permits any non-commercial use, sharing, distribution and reproduction in any medium or format, as long as you give appropriate credit to the original author(s) and the source, provide a link to the Creative Commons licence, and indicate if you modified the licensed material. You do not have permission under this licence to share adapted material derived from this article or parts of it. The images or other third party material in this article are included in the article's Creative Commons licence, unless indicated otherwise in a credit line to the material. If material is not included in the article's Creative Commons licence and your intended use is not permitted by statutory regulation or exceeds the permitted use, you will need to obtain permission directly from the copyright holder. To view a copy of this licence, visit <http://creativecommons.org/licenses/by-nc-nd/4.0/>.

## Introduction

Natural rubber (cis-1,4-polyisoprene; NR) is an essential industrial raw material due to its unique properties, which cannot be fully replaced by synthetic rubbers. Its exceptional resilience, flexibility, wear resistance, heat dissipation, and impact durability make it irreplaceable in numerous applications. In 2018, global NR production reached 13.8 million tons, with Asia accounting for 91.2%, Africa 6.8%, and the Amazon region contributing just 2% of the total. By 2019, NR represented 47.2% of global rubber production, surpassing 13.6 million tons. Almost all commercial NR is derived from the Pará rubber tree (*Hevea brasiliensis* Muell. Arg.), a species native to the Amazon Basin. Today, it is widely cultivated in tropical regions around the world, and it is also the largest tropical crop planted in Hainan, China [1–3]. Tapping Panel Dryness (TPD) syndrome, characterized by partial or complete cessation of latex flow upon tapping, results in significant annual rubber production losses estimated at 15–20%. Approximately 20–50% of productive trees are affected by TPD across rubber tree-growing regions [4]. First reported a century ago [5], the etiology of TPD remains ambiguous despite numerous hypotheses [6]. The prevailing view suggests TPD as a programmed cell death triggered by intensive tapping and prolonged ethylene stimulation [7–10]. However, TPD has also been observed in untapped or newly tapped trees, continuing the search for its causal agent [11, 12]. Viruses have been implicated in causing bark cracking in rubber trees [13], with viroids proposed as associated agents of TPD [11]. Although several viruses naturally infect rubber trees, definitive identification of TPD-related pathogens remains elusive [12]. Recently, a virus tentatively named rubber tree virus 1 (RTV1) was isolated from samples with TPD symptoms in Hainan, China, with its complete genome sequenced (RTV1-QH, MN047299) [14].

RTV1 possesses a 6811-nt positive-sense, single-stranded RNA genome encoding two open reading frames (ORFs). ORF1 (nt 88–6735) encodes a putative 253.7-kDa polyprotein sharing 37% amino acid sequence identity with cherry virus A (*Capillovirus alphavii*; CVA, ARQ83874.1) polyprotein over 99% coverage [15]. The polyprotein includes four domains: methyltransferase (Mtr; aa residues 42–358), RNA helicase (helicase; aa residues 800–1080), RNA-dependent RNA polymerase (RdRp; aa residues 1232–1587), and trichovirus coat protein (CP; aa residues 2052–2206). ORF2 (nt 5055–6437) is predicted to encode a movement protein (MP) sharing 28% amino acid sequence identity (99% coverage) with CVA movement protein (ARQ83899.1) and 36% identity with currant virus A (*Capillovirus alphasibirica*; CuVA, YP\_009229913) [14, 16]. Phylogenetic analysis and genome structure classified RTV1 as a member of the genus *Capillovirus* of the family *Betaflexiviridae* [14].

Other capilloviruses caused severe symptoms in their hosts, such as apple stem grooving virus (*Capillovirus mali*, ASGV), which causes xylem pitting and grooving, phloem necrosis, and reduced productivity in certain apple cultivars [17] and also infects citrus, causing tatter leaf disease [18]. CVA has been found in various hosts like sour cherries, apricots, plums, peaches, and Japanese apricots, often complicating symptom attribution due to frequent mixed infections [19]. Mume virus A (*Capillovirus mume*, MuVA), identified in Japanese apricots, is associated with diffuse chlorotic spots on leaves [20], while loquat virus A (*Capillovirus alphaeribotryae*, LoVA) was detected in a leaf-curling sample from a loquat tree [21]. CuVA discovered in red currants has unclear pathogenicity [16, 22]. Unlike most capilloviruses causing identifiable symptoms in woody plants, the symptoms associated with RTV1 in TPD-affected trees remain unknown and warrant investigation [14].

Previous attempts to associate TPD with RTV1 showed contradictory results: some samples from trees affected by TPD were RTV1-negative in RT-PCR but RTV1-positive in Western blot (WB) using polyclonal antibodies against RTV1-CP (unpublished data). This inconsistency suggests that the genetic diversity of RTV1 may hinder detection via RT-PCR due to mismatches with PCR primers and RTV1 genome sequences. However, there is no data on the genomic diversity of RTV1. In this study, we applied high-throughput sequencing (HTS) combined with RT-PCR amplification to detect RTV1 in samples from different sites in Hainan, China. The sequences presented here highlight RTV1 genetic diversity and indicate the existence of phylogroups within the RTV1 population, which may affect PCR-based diagnosis and may provide insights into the epidemiological and evolutionary relationships of RTV1 populations.

## Materials and methods

### Samples with TPD symptoms collected for RNA-Seq and RT-PCR

Bark and leaf samples from rubber trees showing typical TPD symptoms were collected in various cities in Hainan Province, China (Fig. S1, Table S1). Samples were ground separately in liquid nitrogen. Total RNA from each sample was isolated. RNA-Seq and *de novo* assembly were performed separately for each sample, following previously described methods [23, 24]. Briefly, total RNA was extracted using the RNeasy Plant Plus Kit (TIANGEN BIOTECH, China) according to the manufacturer's instructions. Ribosomal RNA was removed using the Illumina Ribo-Zero rRNA Removal Kit (Plant Leaf). cDNA was synthesized using random hexamer primers and the RevertAid First Strand cDNA Synthesis Kit (Thermo Fisher Scientific), following the manufacturer's instructions. Sequencing and *de novo* assembly

were conducted at Novogene Co. (Beijing, China). Unigenes annotated as RTV1 were selected. Gaps and terminal ends were amplified by RT-PCR using PrimeSTAR® GXL DNA Polymerase (TaKaRa, Dalian, China). The PCR products were ligated into the pMD-19T vector (TaKaRa) after incubation with Taq polymerase at 72 °C for 10 min and subjected to Sanger sequencing (Sangon Biotech, Guangzhou). Overlapping sequences were assembled into complete genomes using SeqMan Pro 7.1.0 (DNA-Star Inc., Madison, WI, USA). Conserved primer sets were designed for the detection of RTV1 (Table S2). To identify primer pairs with a broad detection range, all reported primers for detecting RTV1 were compared in silico with the identified RTV1 genome sequences. PCR conditions included 30 cycles of denaturation at 95 °C for 15 s, primer annealing at 60 °C for 20 s, and extension at 72 °C for 1 min (for a 1 kb product), followed by a final extension at 72 °C for 5 min, using the SanTaq Plus PCR Mix (Sangon Biotech, China).

#### Phylogenetic and sequence analysis of RTV1

The nucleotide sequences of the full-length genome, RdRp, CP, and MP of RTV1 isolates obtained in this study and the RTV1-QH isolate previously submitted to GenBank (MN047299) were aligned using ClustalW with default parameters, respectively. Phylogenetic trees were constructed using the neighbor-joining method with MEGA 7.0 as previously described [12].

#### Recombination analysis

Recombination events were analyzed with the Recombination Detection Program (RDP v.4.95) under default conditions, using an alignment of complete RTV1 genome sequences constructed with MAFFT v7 [25].

#### Pairwise identity matrix and distribution plots

Pairwise nucleotide (nt) and amino acid (aa) identity analyses were performed for 41 RTV1 isolates using the Sequence Demarcation Tool Version 1.3 (SDTv1.3) under default settings [26].

## Results

#### RNA-Seq and *de novo* assembly

Twenty-one bark samples from rubber trees showing TPD symptoms (complete cessation of latex drainage upon tapping) and one symptomless control (DZBYCK) were subjected to RNA extraction and RNA-Seq (Table S1 and Fig. S1). Each RNA-Seq generated approximately 20 million clean reads and 6G clean bases. Following *de novo* assembly of the sequence reads using Trinity, with an overlap length of k-mer = 25 [23, 27], BlastN and BlastX analyses (cut-off value =  $10^{-3}$ ) revealed RTV1 unigenes in 14 symptomatic samples. Most assembled RTV1 unigenes were longer than 6,000 nt, covering almost the complete genome sequence of RTV1 (6,811 nt). However, RTV1 unigenes in some samples were only several hundred nt long, suggesting either a lower RTV1 titer in those samples or insufficient sequencing coverage (Table 1).

To further evaluate the detection capacity of RNA-Seq for RTV1, 8 symptomatic samples that were RTV1-negative in RNA-Seq were tested by Western blot analysis using a polyclonal antibody against RTV1-CP. Seven of the eight samples were negative while one sample was positive for RTV1 (Fig. S2), suggesting that RNA-Seq with 20 million clean reads and 6G clean bases may not entirely ensure detection of RTV1 in bark samples.

Using the unigenes as templates, gaps and terminal ends of the full genome sequences were determined by

**Table 1** Summary of the RNA-Seq, *de novo* assembly, and RTV1 isolates data of bark samples from trees affected by TPD

Sample name	Clean reads	Clean bases	Q30 (%)	GC (%)	Unigenes	RTV1 Unigenes	Longest RTV1 Unigenes	RTV1 isolates identified
DZBYCK	21,022,644	6.31G	92.33	43.09	27,629	0		
DZXQ1	20,462,824	6.14G	92.17	42.5	29,427	2	6757	DZXQ1-1, DZXQ1-2, DZXQ1-3
DZXQ3	20,118,418	6.04G	92.48	44.92	26,137	2	6751	DZXQ3-1, DZXQ3-2, DZXQ3-3
DZXH	21,255,595	6.38G	92.39	42.2	31,694	1	6743	DZXH
DZXQ5	112,702,386	6.54G	93	41.13	28,117	3	6756	DZXQ5
DZXQ6	20,570,697	6.17G	92.46	42.66	29,528	2	6750	DZXQ6
DZXQ7-1	21,083,634	6.33G	92.82	42.13	31,115	2	6802	DZXQ7-1
DZXQ8-1	21,495,780	6.45G	93.06	43.01	32,177	3	652	DZXQ8-1
DZPY1	21,056,452	6.32G	93.09	43.53	35,112	2	6771	DZPY1-1, DZPY1-2, DZPY1-3
DZPY2	21,283,383	6.39G	92.5	42.76	32,979	1	6713	DZPY2
DZPL1	20,997,421	6.3G	92.55	42.68	39,979	4	4598	DZPL1
DZPL2	21,400,745	6.42G	91.97	42.79	30,941	1	373	DZPL2
DZHK	21,234,088	6.37G	91.63	41.87	30,422	1	440	DZHK
DZQN	21,492,493	6.45G	91.83	41.78	32,665	2	914	DZQN
DZCC	21,284,223	6.39G	92.31	42.23	33,371	1	6823	DZCC

RT-PCR, and overlapping sequences were confirmed by Sanger sequencing. In total, 20 new complete genome sequences of RTV1 isolates were identified. Interestingly, three samples (DZXQ1, DZXQ3, and DZPY1) contained more than one RTV1 isolates in the same sample, showing significant variation in nucleotide sequences (Table S1). All isolates shared identical genome organization as the previously reported RTV1-QH isolate, with a 6,811 nt genome (Li et al., 2020), including an 87 nt 5'-UTR, a 76 nt 3'-UTR, and encoding two ORFs.

#### Identification of RTV1 genome via RT-PCR

Alignment analysis revealed highly conserved 3'-UTR sequences among all identified RTV1 isolates, although the coding regions and the 5'-UTR showed significant variation (Fig. 1). One degenerate primer set (RTV1-1 F and RTV1-1R) was designed for direct amplification of the full-length RTV1 genome via RT-PCR (Table S2). Using this primer set, 20 complete RTV1 genomes were identified directly from 48 samples collected from different sites. The newly identified 40 complete genome sequences of RTV1 have been deposited in GenBank under accession numbers PP955903-PP955942.

#### Sequence similarity of the RTV1 isolates

All newly identified RTV1 isolates shared identical genomic length and structure. Compared with the previous RTV1 isolate (RTV1-QH, MN047299), five isolates (DZXQ1-2, CJS LZ, CMFS, CMJJ, and LGRMFY) showed higher genome nucleotide (nt) identity (>90%), while the other thirty-five isolates showed 80–90% nt identity. The most pronounced sequence variation was observed in the RdRp coding region, whereas the CP region maintained the highest similarity in both nucleotide and amino acid (Table 2). Despite notable nucleotide variation (83.44% average identity), amino acid sequences encoding RdRp in these isolates remained highly conserved (92.27% average identity). Notably, the CMJJ isolate displayed the highest sequence homology with the RTV1-QH isolate, with its amino acid sequences of MP and CP sharing 100% identity. Unexpectedly, most RTV1 isolates showed significantly higher nucleotide similarity (91.67% average identity), but lower amino acid similarity (78.22% average identity) in the MP region. Intriguingly, mixed infections involving different RTV1 isolates were discerned in several samples, showing significant variation in the nucleotide sequences (Table 2).

Conserved sequences in the 5'-UTR and 3'-UTR have been used as primers (RTV1-1 F and RTV1-1R) for direct amplification of the full-length RTV1 genome (Fig. 1, Table S2). The Sequence Demarcation Tool (SDT) generates pairwise matrices and identity distribution plots, offering intuitive insights into the relationships among the 41 RTV1 isolates based on nucleotide (nt) and amino

acid (aa) sequences. The pairwise matrices and identity distribution plots revealed significant nt sequence variation among isolates in the RdRp, CP, and complete genomes (Fig. S4), while such variation was less pronounced in the aa sequences (Fig. S5). To facilitate diagnosis of various RTV1 isolates, PCR primers for wider detection range were designed. In silico comparisons were conducted for genome sequences of all 41 RTV1 isolates. Several conserved short fragments among all 41 RTV1 isolates were identified in areas encoding MP and CP. Three PCR primer pairs (RTV1-2 F, RTV1-2R; RTV1-3 F, RTV1-3R; and RTV1-4 F, RTV1-4R) were designed (Table S2). Finally, twenty-two samples from trees affected by TPD collected for RNA-Seq were verified by RT-PCR using these primers. RT-PCR with each primer pair detected RTV1 in at least 12 TPD samples, and overall, RTV1 was detected in 14 samples (Fig. S6), consistent with RNA-Seq and Western-blot results, indicating the reliability of these primers for detection.

#### Phylogenetic analysis of RTV1 isolates

To reveal the genetic diversity and evolutionary relationships of the RTV1 isolates, phylogenetic trees were constructed using either full-genome or RdRp, CP, MP nt sequences (Fig. 2). In the phylogenetic tree constructed from full-genome nt sequences, isolates were clustered into three phylogroups. The largest phylogroup (phylogroup A) included 26 RTV1 isolates, and is prevalent across almost all collection sites (Fig. 2A and Fig. S1). The second large phylogroup B included 12 members, including the RTV1-QH isolate. The locations of both phylogroups overlapped (Fig. S1). Phylogroup C included only three members isolated from two collection sites, Qiongzhou and Danzhou.

Phylogenetic trees based on RdRp, MP, and CP nt sequences were also constructed. Phylogenetic trees based on RdRp sequences delineated similar phylogroup clustering (Fig. 2B), indicating that sequence variation in RdRp represents the genetic diversity among RTV1 isolates. Phylogenetic trees based on MP and CP sequences also generated three phylogroups, but the shorter genetic distances among different phylogroups indicates more similar MP and CP sequences (Fig. 2C-D).

#### Recombination analysis

Recombination analysis was performed with RDP4 using different algorithms (RDP, GENECONV, BootScan, MaxChi, Chimaera, and 3Seq) on an alignment of all full-length RTV1 genome sequences [25]. No recombination events were detected among 41 RTV1 isolates across different phylogroups. Then, recombination events were investigated among isolates within each phylogroup. Ten recombination events were detected among 26 isolates in phylogroup A (Table 3 and Table S3). There was no

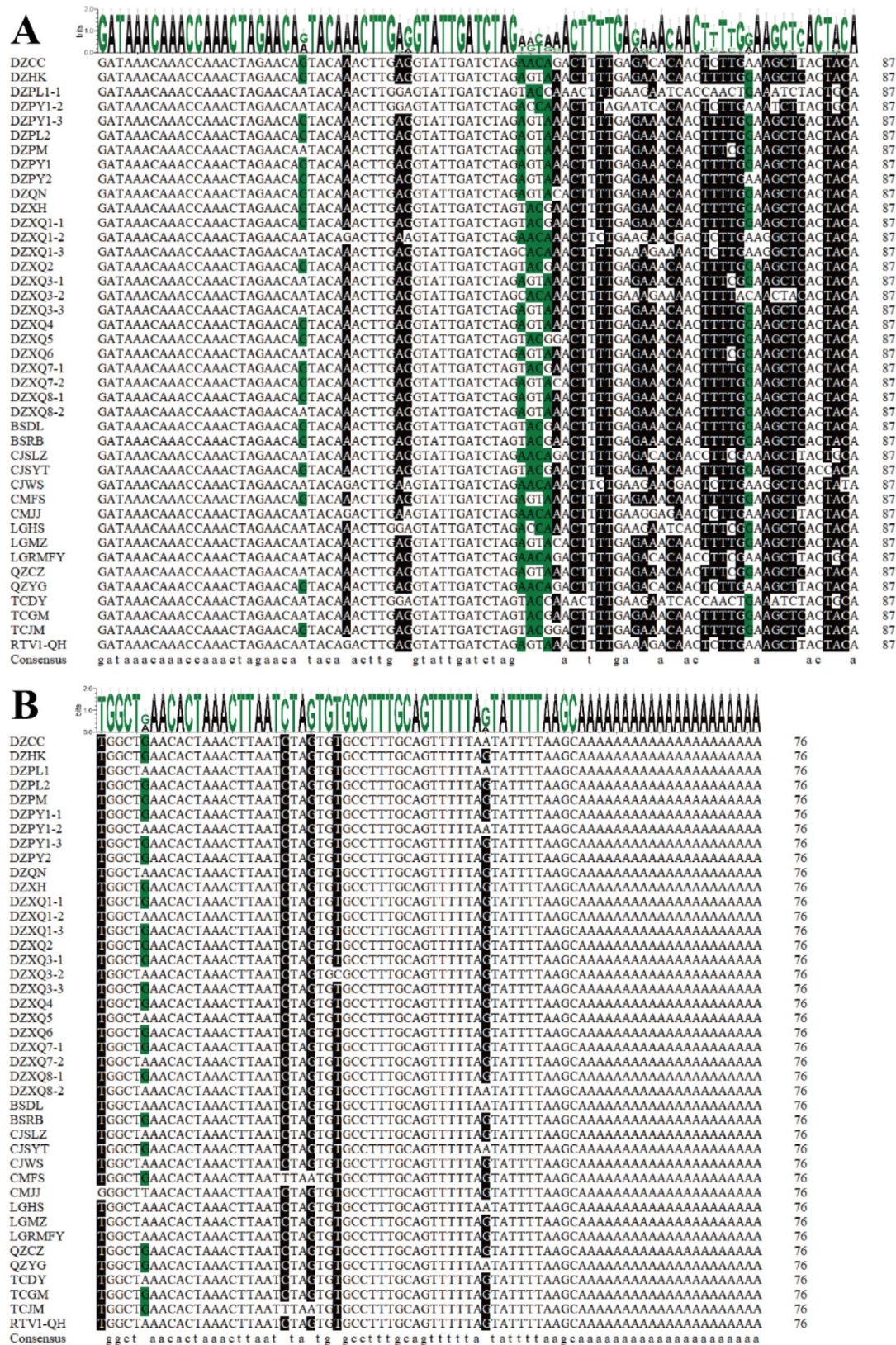


Fig. 1 Alignment of the 5' untranslated region (UTR) and the 3'-UTR

**Table 2** Nucleotide (amino acid) identity (%) between RTV1-QH and the new RTV1 isolates

Isolates	Accession No	Full genome	RdRp	MP	CP
DZXQ1-1	PP955903	82.93(85.81)	83.72(92.41)	90.40(74.10)	90.34(98.60)
DZXQ1-2	PP955904	90.40(93.32)	89.19(93.46)	96.20(89.88)	94.17(99.40)
DZXQ1-3	PP955905	81.30(84.52)	74.70(84.52)	89.00(73.71)	90.18(97.82)
DZXQ2	PP955906	82.93(85.81)	83.72(92.41)	90.40(74.10)	90.34(98.60)
DZXQ3-1	PP955907	82.80(86.08)	83.28(92.08)	89.80(72.29)	90.18(99.07)
DZXQ3-2	PP955908	80.93(87.12)	74.72(85.20)	89.00(75.61)	86.96(98.60)
DZXQ3-3	PP955909	82.83(85.83)	76.85(86.85)	90.80(78.52)	90.18(96.72)
DZXQ4	PP955910	82.67(85.86)	83.50(92.08)	90.40(74.10)	90.34(99.07)
DZXQ5	PP955911	82.81(85.95)	83.72(92.41)	90.40(74.10)	90.03(99.53)
DZXH	PP955912	82.71(85.81)	83.50(92.08)	90.60(74.70)	90.49(99.07)
DZXQ6	PP955913	82.80(86.61)	82.95(91.75)	89.80(72.29)	90.18(99.07)
DZXQ7-1	PP955914	82.71(86.26)	83.17(91.75)	90.60(74.70)	90.49(99.07)
DZXQ7-2	PP955915	82.81(86.48)	83.39(92.08)	90.40(74.10)	90.03(99.07)
DZXQ8-1	PP955916	82.67(86.34)	83.17(91.75)	90.40(74.10)	90.34(99.07)
DZXQ8-2	PP955917	82.42(86.96)	82.73(90.76)	90.00(72.89)	91.41(99.53)
DZPY1-1	PP955918	82.93(86.43)	83.06(91.75)	90.40(74.10)	90.34(98.60)
DZPY1-2	PP955919	81.52(85.10)	77.33(88.90)	90.40(75.52)	89.88(96.87)
DZPY1-3	PP955920	83.07(86.10)	80.89(91.68)	90.40(78.63)	90.34(97.52)
DZPY2	PP955921	82.67(86.34)	83.17(91.75)	90.40(74.10)	90.34(99.07)
DZPL1	PP955922	81.38(85.24)	73.49(83.50)	90.40(73.49)	90.03(99.07)
DZPL2	PP955923	82.93(86.43)	83.06(91.75)	90.40(74.10)	90.34(98.60)
DZHK	PP955924	82.71(86.39)	83.17(91.75)	90.60(74.70)	90.49(99.07)
DZPM	PP955925	82.80(86.30)	82.95(91.75)	89.80(74.70)	90.18(99.07)
DZQN	PP955926	82.81(86.48)	83.39(92.08)	90.40(74.10)	90.03(99.07)
DZCC	PP955927	82.60(86.12)	83.17(91.42)	89.60(74.49)	90.18(98.60)
BSDL	PP955928	81.21(84.98)	73.38(83.83)	90.40(73.49)	89.88(99.07)
BSRB	PP955929	83.93(86.52)	83.61(92.41)	90.40(74.10)	94.63(99.53)
CJSLZ	PP955930	90.74(93.05)	91.41(97.03)	95.60(88.55)	93.56(99.53)
CJSYT	PP955931	82.71(85.81)	83.72(92.08)	90.60(74.70)	90.18(99.07)
CJWS	PP955932	89.29(94.05)	88.89(97.36)	96.00(90.36)	94.48(98.60)
CMFS	PP955933	95.38(97.58)	98.02(98.02)	99.00(97.59)	90.18(99.07)
CMJJ	PP955934	93.56(96.26)	98.90(98.68)	99.80(100.0)	98.16(100.0)
LGHS	PP955935	81.48(85.42)	80.86(92.41)	90.40(73.49)	90.18(99.07)
LGMZ	PP955936	83.50(83.36)	80.86(92.41)	90.80(75.30)	88.34(99.07)
LGRMFY	PP955937	90.52(93.44)	90.98(96.70)	96.80(92.17)	93.40(99.53)
QZCZ	PP955938	80.61(86.61)	82.95(91.75)	88.80(70.48)	90.18(98.14)
QZYG	PP955939	80.81(86.17)	83.17(99.01)	88.80(70.48)	90.18(99.07)
TCDY	PP955940	87.83(90.57)	88.82(92.74)	99.60(100.0)	95.55(99.53)
TCGM	PP955941	82.79(85.95)	83.06(99.01)	90.80(75.30)	90.18(98.60)
TCJM	PP955942	83.90(88.81)	83.17(99.34)	98.00(95.78)	90.18(99.07)
Average		83.99(87.46)	83.44(92.27)	91.67(78.22)	90.93(98.87)

evident correlation between geographical distance and recombination events. Further investigation of recombination events in isolates BSRB and TCJM showed events at the MP and CP region, suggesting close correlation of recombination events with higher sequence similarity.

## Discussion

To date, there have been five reports of virus infection in rubber trees. However, it remains unconfirmed whether these viruses are associated with TPD [12]. The first virus ever recorded to infect rubber trees belongs to the family

*Betaflexiviridae*, specifically the genus *Carlavirus*. It was discovered in seedlings that exhibited inter-veinal chlorosis [28]. The second putative virus, named *Hevea brasiliensis* virus (HBrV), was identified in asymptomatic leaf samples by small RNA sequencing (sRNA-seq), and it is regarded as a latent virus [29]. In 2020, three viruses were found in samples with TPD symptoms through sRNA-seq. Two closely related virga-like viruses, namely rubber tree latent virus 1 (RTLTV1) and rubber tree latent virus 2 (RTLTV2) were identified, and the latent infection of both RTLTV1 and RTLTV2 in rubber tree seedlings

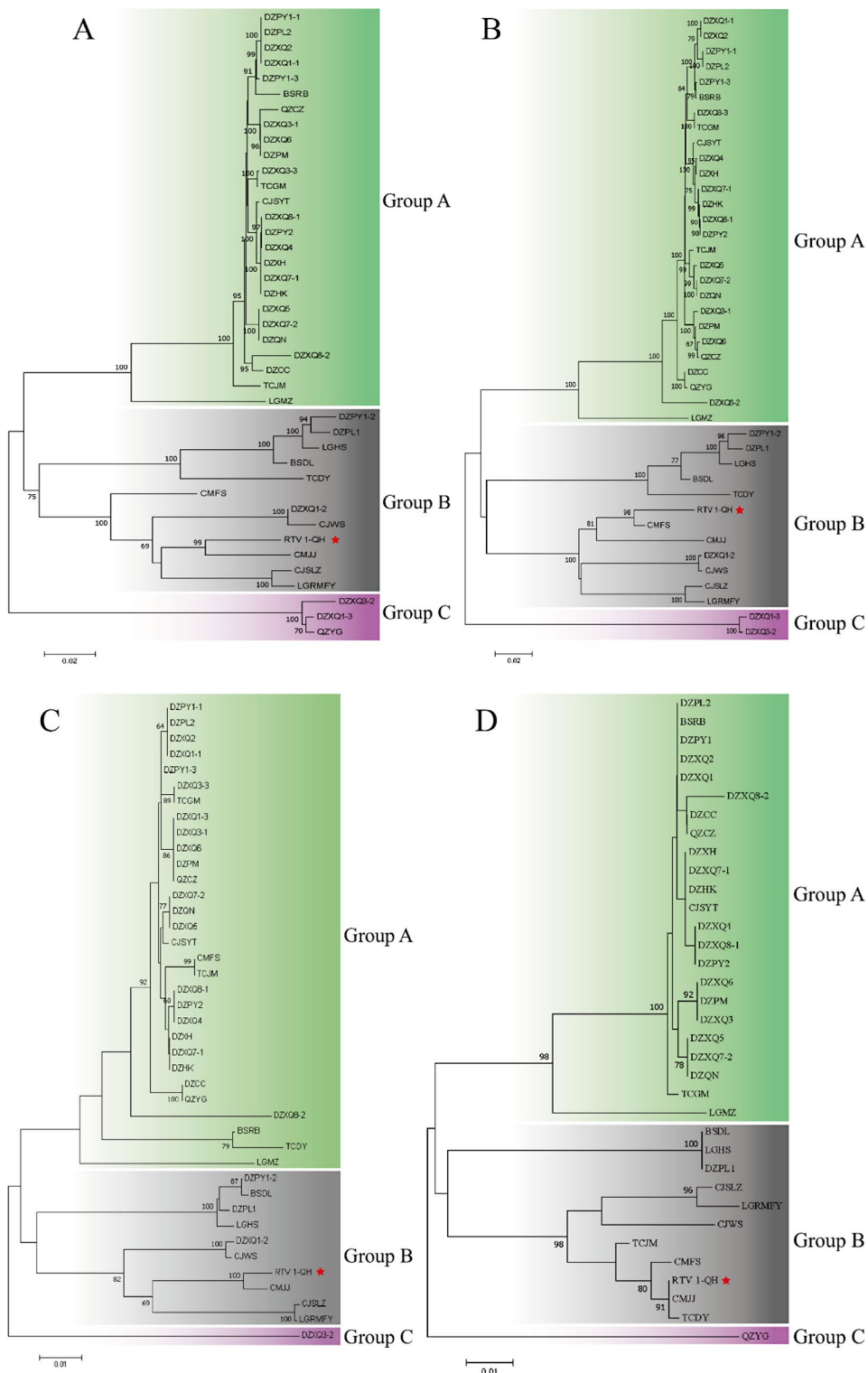


**Fig. 2** Phylogenetic analyses of RTV1 isolates. **(A)** Phylogenetic tree based on the complete genome sequence of RTV1 isolates. **(B)** Phylogenetic tree based on RdRp nucleotide sequences of RTV1 isolates. **(C)** Phylogenetic tree based on CP nucleotide sequences of RTV1 isolates. **(D)** Phylogenetic tree based on MP nucleotide sequences of RTV1 isolates

**Table 3** Recombination events predicted by RDP4 in the full genomes of the RTV1 isolates from phylogroup A

Event No.	Recombination	Major parent	Minor parent	Recombination analysis	
				Detection methods	P-value
1	BSRB	DZPT1-3	Unknow(DZXQ8-2)	<u>RGMC</u> T	1.002E-40
2	TCJM	DZQN	Unknow(DZXQ8-2)	<u>RGMC</u> T	4.835E-34
3	BSRB	TCJM	DZQN	<u>T</u>	1.83E-06
4	DZCC	DZXQ	Unknow(DZPY2)	<u>R</u> G	7.15E-05
5	LGMZ	Unknow(DZXQ8-2)	QZCZ	<u>R</u> MC	6.45E-07
6	LGMZ	Unknow(DZXQ3-3)	DZXQ8-2	<u>G</u>	8.27E-06
7	DZXQ8-2	DZXQ3-3	Unknow(LGMZ)	<u>M</u>	4.54E-05
8	DZCZ	TCJM	BSRB	<u>T</u>	1.58E-03
9	DZCZ	DZPY	Unknow(DZXQ8-2)	<u>G</u>	2.16E-02
10	DZQN	TCJM	CISYT	<u>T</u>	3.44E-02

Minor Parent: Parent contributing smaller fraction of sequence; Major Parent: Parent contributing larger fraction of sequence; Unknown: Only one parent and a recombinant need to be in the alignment for a recombination event to be detectable. Recombination detection methods used are: R-RDP; G-GENCONV; M-MAXCHI; C-CHIMERA; T-3SEQ. The lowest p-value detected by the underlined method mentioned in the previous column was shown.

was confirmed [12, 30]. Another virus, RTV1, was documented as a member of the genus *Capillovirus* within the family *Betaflexiviridae* [14], with only one complete genome sequence deposited in GenBank to date. The lack of genetic variability data for RTV1 has hindered the design of conserved PCR primers for RTV1 diagnosis and the study of its pathogenicity. In this study, we conducted transcriptomic analysis on 22 samples with TPD syndrome, of which 15 samples (including one sample identified by WB) were found to be infected with RTV1. We successfully obtained complete genomes of 20 RTV1 isolates through *de novo* assembly and RT-PCR verification. Additionally, 20 complete RTV1 genomes were cloned directly via RT-PCR using conserved sequences from UTR regions as primers. Thus, only approximately 50% of the samples with TPD syndrome collected in Hainan, China, were found to be infected with RTV1. While it is possible that some RTV1 isolates evaded RNA-seq and RT-PCR detection, it can be concluded that not all samples were infected with RTV1, suggesting that RTV1 may not be the causal agent of TPD. However, the term “TPD syndrome” has been widely used to describe the phenomenon of latex flow cessation upon tapping in rubber trees. Many studies have proposed that TPD represents a form of programmed cell death resulting from prolonged tapping and ethylene stimulation [7–9]. Chrestin et al. categorized TPD into reversible physiological responses to overexploitation and irreversible bark necrosis (BN) [31–33]. Various viroid-like RNAs (250–400 nucleotides) and double-stranded virus-like RNAs (1,800 bp) have been identified in bark necrosis (BN) [11, 33], but no definitive biotic causal agent has been correlated with BN. Whether RTV1 is a causal agent of bark necrosis requires further investigation. It is therefore crucial to investigate which symptoms are associated with RTV1 infection.

The conserved degenerate primer sets designed for RTV1 detection in this study may prove useful for future investigations. To enhance detection accuracy, PCR detection should be combined with serological methods such as Western-blot and ELISA [34, 35].

Recent studies have explored the genomic diversity of other viruses within the *Capillovirus* genus, including investigations into ASGV [36], CVA [37], and MuVA [38]. In ASGV, the coat protein (CP) is the most conserved part of the virus genome, while ORF1, encoding a polyprotein involved in virus replication, shows regions of high variability [18, 39, 40]. CVA virus isolates also exhibit substantial genome sequence diversity, particularly within the RdRp nucleotides and amino acids, whereas sequences for CP and MP remain relatively conserved [37, 41]. Similarly, as shown in this study, RTV1 displays considerable genetic diversity, with 81.92–99.98% pairwise sequence identities among the 41 isolates (Fig. S4). The RTV1 genome exhibits notable variation in the sequence encoding the RdRp domain, while conserved sequences are observed in the regions encoding MP and CP (Table 2 and Fig. S5), indicating that MP and CP are conserved proteins within the *Capillovirus* genus. Additionally, co-infections involving different RTV1 phylogroups were observed within the same host, a phenomenon documented in various viruses and their hosts [42–45].

In the phylogenetic trees constructed based on the full-genome, RdRp, CP, and MP nt sequences, the isolates were grouped into three phylogroups. Most of the isolates (67.5%) from Danzhou city were clustered to phylogroup A, while the remaining isolates were assigned to phylogroup B and C (Fig. 2), implying that phylogroup A exhibited the highest prevalence. The phylogenetic clustering of RTV1 isolates did not indicate a

close association with geographical origin (Fig. 2 and S1). RDP4 analysis identified 10 recombination events among phylogroup A RTV1 isolates, which were not evidently correlated with geographical distance. The evolutionary relationships among RTV1 isolates remain complex. ASGV diversity has been found to be structured more by host plant species than by geographical origin [39]. The heightened genomic variability of ASGV may arise from recombination events between isolates infecting diverse host species [40]. However, the rubber tree is currently the only known host of RTV1. Further investigation is needed to determine whether there are other hosts of RTV1 in the surrounding environment of rubber trees.

### Supplementary Information

The online version contains supplementary material available at <https://doi.org/10.1186/s12864-025-11305-6>.

Supplementary Material 1

### Author contributions

X.C., X.H. and H.W. have conceived and designed the experiments; H.W. and R.Z. performed the experiments; H.W. and X.C. analyzed the data; X.C. wrote the paper; R.Z. and X.H. revised the paper. All authors discussed the results and contributed to the final manuscript.

### Funding

This study was supported financially by the Hainan Major Research Project for Science and Technology (grant no. ZDYF2024XDNY208).

### Data availability

The complete RTV1 genome sequences were deposited in GenBank with respective accession numbers PP955903-PP955942 and the datasets used and/or analyzed during the current study available from the corresponding author on reasonable request.

### Declarations

#### Ethics approval and consent to participate

This study did not include the use of any animals, human or otherwise, so did not require ethical approval. The collection of leaf samples and use in the study are complying with relevant institutional, national, and international guidelines.

#### Consent for publication

Not applicable.

#### Competing interests

The authors declare no competing interests.

Received: 27 June 2024 / Accepted: 29 January 2025

Published online: 12 February 2025

### References

- Nakano Y, Mitsuda N, Ide K, Mori T, Mira FR, Rosmalawati S, Watanabe N, Suzuki K. Transcriptome analysis of Pará rubber tree (*H. brasiliensis*) seedlings under ethylene stimulation. *BMC Plant Biol.* 2021;21(1):420.
- Florez-Velasco N, Ramos VF, Magnitskiy S, Balaguera-López HJAA. Ethylene and jasmonate as stimulants of latex yield in rubber trees (*Hevea brasiliensis*): molecular and physiological mechanisms. A systematic approximation review. *Adv Agrochem.* 2024;3:279–88.
- HE C, LIU R, AN F, WU W, LIU D. Analysis of Renewal Strategies of Natural Rubber Plantations in Hainan Province. *China Trop Agric.* 2024;5(120):9–18.
- de Faj EJAJB. Histo-and cytopathology of trunk phloem necrosis, a form of rubber tree (*Hevea brasiliensis* Müll. Arg.) Tapping panel dryness. 2011;59(6):563–74.
- Chandler SE. The Brown Bast Disease of the Para Rubber-Tree. *Nature.* 1922;109(2733):357–60.
- Qin B-X, Hu X-W, Deng X-D, Guo J-C. Mechanism and formation of tapping panel dryness Symptom in *Hevea*. *Plant Physiol J.* 2005;41(5):827–30.
- Nie Z, Kang G, Yan D, Qin H, Yang L, Zeng R. Downregulation of HbFPS1 affects rubber biosynthesis of *Hevea brasiliensis* suffering from tapping panel dryness. *Plant Journal: Cell Mol Biology.* 2023;113(3):504–20.
- Lestari D, Endang TP. Rubber Exploitation System and Its Influence on Tapping Panel Dryness Disease (Case Study: PT Perkebunan Nusantara XII Kebun Kotta Blater). *Nusantara Science and Technology Proceedings.* 2023;28–31.
- Liu H, Wei Y, Deng Z, Yang H, Dai L, Li D. Involvement of HbMC1-mediated cell death in tapping panel dryness of rubber tree (*Hevea brasiliensis*). *Tree Physiol.* 2019;39(3):391–403.
- Zhang Y, Leclercq J, Montoro P. Reactive oxygen species in *Hevea brasiliensis* latex and relevance to tapping panel dryness. *Tree Physiol.* 2017;37(2):261–9.
- Ramachandran P, Mathur S, Francis L, Varma A, Mathew J, Mathew NM, Sethuraj MR. Evidence for Association of a viroid with tapping panel dryness syndrome of Rubber (*Hevea brasiliensis*). *Plant Dis.* 2000;84(10):1155.
- Zhao R, Su X, Yu F, Liu Z, Huang X. Identification and characterization of two closely related virga-like viruses latently infecting rubber trees (*Hevea brasiliensis*). *Front Microbiol.* 2023;14:1286369.
- Peries OS, Brohier YEM. A virus as the causal agent of bark cracking in *Hevea brasiliensis*. *Nature.* 1965;205(4971):624–5.
- Li Z, Wang H, Zhao R, Zhang Z, Xia Z, Zhai J, Huang X. Complete genome sequence of a novel capillovirus infecting *Hevea brasiliensis* in China. *Arch Virol.* 2020;165(1):249–52.
- Kesanakurti P, Belton M, Saeed H, Rast H, Boyes I, Rott M. Comparative analysis of cherry virus a genome sequences assembled from deep sequencing data. *Arch Virol.* 2017;162(9):2821–8.
- Petrzik K, Přibylková J, Koloniuk I, Špak J. Molecular characterization of a novel capillovirus from red currant. *Arch Virol.* 2016;161(4):1083–6.
- Shokri S, Shujaei K, Gibbs AJ, Hajizadeh M. Evolution and biogeography of apple stem grooving virus. *Virus J.* 2023;20(1):105.
- Magome H, Yoshikawa N, Takahashi T, Ito T, Miyakawa T. Molecular variability of the genomes of capilloviruses from apple, Japanese pear, European pear, and citrus trees. *Phytopathology.* 1997;87(4):389–96.
- Ben Mansour K, Komínek P, Komínková M, Brožová J. Characterization of Prunus Necrotic Ringspot Virus and Cherry Virus A Infecting Myrobalan Rootstock. *Viruses.* 2023;15(8):1723.
- Zheng Y, Bu F, Wu C, Chen J, Liu Z, Xiang B. Cui BJPD: First Report of Mume Virus A infection of *Prunus persica* in China. *Plant Dis.* 2020;104(10):2741.
- Liu Q, Yang L, Xuan Z, Wu J, Qiu Y, Zhang S, Wu D, Zhou C, Cao M. Complete nucleotide sequence of loquat virus A, a member of the family Betaflexiviridae with a novel genome organization. *Arch Virol.* 2020;165(1):223–6.
- Marais A, Faure C, Theil S, Candresse T. Molecular Characterization of a Novel Species of Capillovirus from Japanese Apricot (*Prunus mume*). *Viruses* 2018;10(4):144.
- Cao X, Zhao R, Wang H, Zhang H, Zhao X, Khan LU, Huang X. Genomic diversity of Areca Palm Velarivirus 1 (APV1) in Areca palm (*Areca catechu*) plantations in Hainan, China. *BMC Genomics.* 2021;22(1):725.
- Wang H, Zhao R, Zhang H, Cao X, Li Z, Zhang Z, Zhai J, Huang X. Prevalence of yellow leaf disease (YLD) and its associated areca palm velarivirus 1 (APV1) in betel palm (*Areca catechu*) plantations in Hainan, China. *Plant Dis.* 2020;104(10):2556–62.
- Martin DP, Murrell B, Golden M, Khoosal A, Muhire B. RDP4: detection and analysis of recombination patterns in virus genomes. *Virus Evol.* 2015;1(1):vev003.
- Kuhn JH, Muhire BM, Varsani A, Martin DP. SDT: a virus classification Tool based on pairwise sequence alignment and identity calculation. *PLoS ONE.* 2014;9(9):e108277.
- Grabherr MG, Haas BJ, Yassour M, Levin JZ, Thompson DA, Amit I, Adiconis X, Fan L, Raychowdhury R, Zeng Q, et al. Full-length transcriptome assembly from RNA-Seq data without a reference genome. *Nat Biotechnol.* 2011;29(7):644–52.
- Gama M, Kitajima E, Ávila A, Lin M. Um Carlavírus em seringueira (*Hevea brasiliensis*). *Fitopatol Bras.* 1983;3:621.

29. Fonseca PLC, Badotti F, de Oliveira TFP, Fonseca A, Vaz ABM, Tomé LMR, Abrahão JS, Marques JT, Trindade GS, Chaverri P, et al. Virome analyses of *Hevea brasiliensis* using small RNA deep sequencing and PCR techniques reveal the presence of a potential new virus. *Virology*. 2018;15(1):184.
30. Chen S, Yu F, Li Z, Zhang Y, Wang H, Zhai J, Huang X. Complete genome sequence of a novel virga-like virus infecting *Hevea brasiliensis*. *Arch Virol*. 2022;167(3):965–8.
31. Chrestin H, Sookmark U, Trouslot P, Pellegrin F, Nandris D. Rubber Tree (*Hevea brasiliensis*) bark necrosis syndrome III: a physiological disease linked to impaired cyanide metabolism. *Plant Dis*. 2004;88(9):1047.
32. Nandris D, Moreau R, Pellegrin F, Chrestin H, Abina J, Angui P. Rubber Tree (*Hevea brasiliensis*) bark necrosis syndrome II: First Comprehensive Report on Causal stresses. *Plant Dis*. 2004;88(9):1047.
33. Pellegrin F, Nandris D, Chrestin H, Duran-Vila N. Rubber Tree (*Hevea brasiliensis*) bark necrosis syndrome I: still no evidence of a biotic Causal Agent. *Plant Dis*. 2004;88(9):1046.
34. Niu Y, Wang D, Cui L, Wang B, Pang X, Yu P. Monoclonal antibody-based colloidal gold immunochromatographic strip for the rapid detection of Tomato zongonate spot tospovirus. *Virology*. 2018;15(1):15.
35. Ren R, Wang T, Gao L, Song P, Yang Y, Zhi H, Li K. Development of Comprehensive Serological techniques for sensitive, quantitative and Rapid Detection of Soybean mosaic virus. *Int J Mol Sci*. 2022;23(16):9457.
36. Jo Y, Choi H, Kim SM, Kim SL, Lee BC, Cho WK. Integrated analyses using RNA-Seq data reveal viral genomes, single nucleotide variations, the phylogenetic relationship, and recombination for Apple stem grooving virus. *BMC Genomics*. 2016;17:579.
37. Gao R, Xu Y, Candresse T, He Z, Li S, Ma Y, Lu M. Further insight into genetic variation and haplotype diversity of Cherry virus A from China. *PLoS ONE*. 2017;12(10):e0186273.
38. Lee J, Lee DS, Ryu H, Lim S, Lee SJ. First report of mume virus A infecting *Prunus salicina* worldwide and *Prunus mume* in Korea. *Plant Dis*. 2022;107:972.
39. Liebenberg A, Moury B, Sabath N, Hell R, Kappis A, Jarusch W, Wetzel T. Molecular evolution of the genomic RNA of Apple stem grooving capillivirus. *J Mol Evol*. 2012;75(3–4):92–101.
40. Chen H, Chen S, Li Y, Ye T, Hao L, Fan Z, Guo L, Zhou T. Phylogenetic analysis and recombination events in full genome sequences of apple stem grooving virus. *Acta Virol*. 2014;58(4):309–16.
41. Rui G, Li SF, Lu MG. Complete nucleotide sequences of two isolates of Cherry virus A from sweet cherry in China. *J Integr Agric*. 2016;15(7):1667–71.
42. Xu Y, Li S, Na C, Yang L, Lu M. Analyses of virus/viroid communities in nectarine trees by next-generation sequencing and insight into viral synergisms implication in host disease symptoms. *Sci Rep*. 2019;9(1):12261.
43. Tahzima R, Foucart Y, Peusens G, Beliën T, Massart S, De Jonghe K. High-throughput sequencing assists studies in genomic variability and epidemiology of little Cherry Virus 1 and 2 infecting *Prunus* spp. in Belgium. *Viruses*. 2019;11(7):592.
44. Katsiani A, Maliogka VI, Katis N, Svanella-Dumas L, Olmos A, Ruiz-García AB, Marais A, Faure C, Theil S, Lotos L, et al. High-throughput sequencing reveals further diversity of little Cherry Virus 1 with implications for Diagnostics. *Viruses*. 2018;10(7):385.
45. Mulabisana MJ, Cloete M, Laurie SM, Mphela W, Maserumule MM, Nhlapo TF, Cochrane NM, Oelofse D, Rey MEC. Yield evaluation of multiple and co-infections of begomoviruses and potyviruses on sweet potato varieties under field conditions and confirmation of multiple infection by NGS. *Crop Prot*. 2019;119:102–12.

#### Publisher's note

Springer Nature remains neutral with regard to jurisdictional claims in published maps and institutional affiliations.